INTERNATIONAL JOURNAL OF Experimental Pathology

*Int. J. Exp. Path.* (2011), 92, 243–250

ORIGINAL ARTICLE

# Alterations induced by chronic lead exposure on the cells of circadian pacemaker of developing rats

Julio César Rojas-Castañeda*†, Rosa María Vigueras-Villaseñor*, Patricia Rojas‡, Margarita Chávez-Saldaña*, Oscar Gutiérrez- Pérez*, Sergio Montes§ and Camilo Ríos§

*Subdirección de Medicina Experimental, Instituto Nacional de Pediatría, México D.F., México,‡Laboratorio de Neurotoxicología, Instituto Nacional de Neurología y Neurocirugía MVS, México D.F., México,§Departamento de Neuroquímica, Instituto Nacional de Neurología y Neurocirugía MVS, México D.F., México and †Doctorado en Ciencias Biológicas, Universidad Autónoma Metropolitana, México D.F., México

INTERNATIONAL JOURNAL OF EXPERIMENTAL PATHOLOGY

doi: 10.1111/j.1365-2613.2011.00761.x

Received for publication:
31 August 2010
Accepted for publication:
31 December 2010

**Correspondence:**
Julio César Rojas Castañeda
Instituto Nacional de Pediatría
Av. Insurgentes Sur 3700- C
Col. Insurgentes-Cuicuilco
Coyoacán
C.P. 04530
México D.F.
México
Tel.: (+52) (55) 1084 0900, extn:1453
Fax: (+52) (55) 1084 5533
E-mail: rocajc1@yahoo.com.mx

Camilo Ríos
Instituto Nacional de Neurología y Neurocirugía MVS Av. Insurgentes Sur 3877, Col. La Fama, Tlalpan
C.P. 14269, México D.F. México
Tel.: (+52) (55) 5606 3822, extn:2006
Fax: (+52) (55) 5528 0095
E-mail: crios@correo.xoc.uam.mx

## Summary

Lead (Pb) exposure alters the temporal organization of several physiological and behavioural processes in which the suprachiasmatic nucleus (SCN) of the hypothalamus plays a fundamental role. In this study, we evaluated the effects of chronic early Pb exposure (CePbe) on the morphology, cellular density and relative optical density (OD) in the cells of the SCN of male rats. Female Wistar rats were exposed during gestation and lactation to a Pb solution containing 320 ppm of Pb acetate through drinking water. After weaning, the pups were maintained with the same drinking water until sacrificed at 90 days of age. Pb levels in the blood, hypothalamus, hippocampus and prefrontal cortex were significantly increased in the experimental group. Chronic early Pb exposure induced a significant increase in the minor and major axes and somatic area of vasoactive intestinal polypeptide (VIP)- and vasopressin (VP)-immunoreactive neurons. The density of VIP-, VP- and glial fibrillary acidic protein (GFAP)-immunoreactive cells showed a significant decrease in the experimental group. OD analysis showed a significant increase in VIP neurons of the experimental group. The results showed that CePbe induced alterations in the cells of the SCN, as evidenced by modifications in soma morphology, cellular density and OD in circadian pacemaker cells. These findings provide a morphological and cellular basis for deficits in circadian rhythms documented in Pb-exposed animals.

**Keywords**
glial fibrillary acidic protein, lead, relative optical density, suprachiasmatic nucleus, vasoactive intestinal polypeptide, vasopressin

Lead (Pb) is a heavy metal with no apparent biological function. This metal is used in a variety of compounds with multiple applications (Verstraeten *et al.* 2008). This confirms that Pb exposure in human populations still persists and constitutes a significant public health problem, despite efforts to reduce its level in the ecosystem.

The effects of chronic Pb exposure during development of the central nervous system have showed alterations in granule cell neurogenesis and morphology in the hippocampus (Verina *et al.* 2007). In addition, it produces changes in the subunit composition of glutamatergic *N*-methyl-D-aspartate (NMDA) receptors and reduces $Ca^{2+}$/cyclic AMP response

element-binding protein (CREB) phosphorylation in cortical and hippocampal nuclear extracts (Toscano *et al.* 2002). Moreover, it induces apoptosis in hippocampus (Han *et al.* 2007; Kumar *et al.* 2009; Sharifi *et al.* 2010) as well as a decrease in the number of neurons of CA1, CA3 and dentate gyrus regions of the hippocampus (Han *et al.* 2007). The same phenomenon is associated with changes in glutamate and GABA release in the hippocampal CA1 and dentate regions (Lasley & Gilbert 2002) and impairment of learning (Winneke 1996).

Circadian oscillators with intrinsic periods of approximately 24 h enable organisms to anticipate and synchronize (entrains) their physiology and behaviour to periodic changes in the environment. In mammals, a central pacemaker exists in the suprachiasmatic nucleus (SCN) of the hypothalamus, which generates and communicates a circadian rhythm to other parts of the brain and to peripheral tissues. The self-sustained oscillation is generated by the interaction of a set of activated clock genes. These included the transcriptional activators: CLOCK and BMAL1, and repressors: PER1-3, CRY 1-2 and REV-ERVα, and these constitute the transcriptional–translational feedback loop that occurs with near 24-h kinetics (Reppert & Weaver 2002; Hastings & Herzog 2004). However, these are not the only transcription factors for generating intrinsic circadian rhythms. Additional genes have been proposed as circadian clock components (Tho 2008).

The SCN is anatomically divided into shell (dorsomedial) and core (ventrolateral) regions. The shell region cells contain vasopressin (VP) and mostly receive non-photic input. The core subdivision of the SCN contains vasoactive intestinal polypeptide (VIP) immunoreactive neurons and receives direct or indirect photic information from the retina (Yan & Silver 2002; Hastings *et al.* 2007; Karatsoreos & Silver 2007).

The VIP neurons are believed to act as an integrator of external input. They relay this information to the rest of the SCN. VP neurons appear to generate the most robust circadian oscillations (Yan & Okamura 2002).

Studies carried out to analyse the effects of chronic Pb exposure on the circadian timing system showed the existence of alterations in circadian rhythms in rats. An increase in the rhythm of locomotor activity during the light phase (Collins *et al.* 1984) and alterations in the time between the locomotor activity onset and lights-off under the light/dark cycle (which may reflect an alteration in the entrainment to light/dark cycle) (Rojas-Castañeda *et al.* 2007) have been reported. Furthermore, a significant decrease in motor cortex and hippocampus in the alpha and theta band electroencephalogram spectral power in both wakeful and slow wave sleep stages were reported (Kumar & Desiraju 1992). An increase during the light phase in the rhythm of locomotor activity (Shafiq-ur-Rehman *et al.* 1986) and in behavioural patterns such as rearing and preening (Shafiq-ur-Rehman 1999) was observed in rats with acute Pb exposure.

The changes observed in the studies mentioned previously suggest that Pb exposure may affect the structures and/or functions involved in the circadian timing system. However, possible structural changes on the cells of the SCN associated with Pb exposure have not been investigated. This study was designed to establish whether the reported alterations in the circadian rhythms of rats exposed to Pb might be accompanied by changes in SCN morphology. Therefore, we evaluated the effects of exposure to Pb on the morphology of VIP- and VP-immunoreactive neurons, cellular density of VIP-, VP- and glial fibrillary acidic protein (GFAP)-immunoreactive cells and expression of VIP-, VP-and GFAP-proteins using relative optical density (OD) analysis in the middle sections of the SCN of rats with chronic early Pb exposure (CePbe).

## Materials and methods

### *Animals and exposure protocol*

Female (250–275 g) and male (300–325 g) Wistar rats born and bred at the Instituto Nacional de Pediatría were used for breeding. They were maintained with tap water and standard laboratory food *ad libitum* (LabDiet 5001®; PMI Nutrition International, Inc., Brentwood, MO, USA) and housed in a temperature-controlled room (21 ± 1 °C) with relative humidity of 52 ± 10%. The room lighting was set to a 12:12-h light/dark cycle (lights on at 07:00). Vaginal smears were obtained each morning to detect the occurrence of mating determined by the presence of sperm in the smear and showed the beginning of the exposure period.

Pb-exposed pregnant rats received as the only source of beverage a solution containing 320 ppm of Pb acetate (J.T. Baker, Edo. de Mex., Mexico) in tap water during the gestation. Control pregnant rats ingested tap water. To prevent the formation of Pb precipitate, 0.5 ml of glacial acetic acid to prepare 1000 ml of solutions was added to all drinking solutions (Wang *et al.* 2006; Han *et al.* 2007). The pups from both groups were treated after birth in the same way until 90 days of age. This exposure protocol was chosen based on previous studies demonstrating an increase in lipid peroxidation in several brain regions (Villeda-Hernández *et al.* 2001) and alterations in the rhythm of locomotor activity (Rojas-Castañeda *et al.* 2007).

At 21 days of age, pups were weaned to the same drinking water as that given to their dams, housed in groups of four in same-sex colony cages and were maintained on these regimens until sacrifice. All animals were treated humanely to minimize discomfort in accordance with the ethical principles and specified regulations as stated in the Official Mexican Norm NOM-062-2OO-1999 entitled 'Technical specifications for the production, care and use of laboratory animals'. This work was approved by our Institutional Animal Care and Use Committee (Instituto Nacional de Pediatría).

### *Determination of Pb in blood and brain regions*

Pb levels in blood and brain regions (hypothalamus, hippocampus and prefrontal cortex) were analysed by graphite furnace atomic absorption spectrophotometry.

On postnatal day 90, five male rats from each group were randomly selected and anaesthetized with sodium pentobarbital (40 mg/kg, ip; Pfizer, Edo. de Mex., México) between 12:00–13:00 h to prevent circadian fluctuations. Blood samples were obtained for Pb analysis by cardiac puncture in blood collection tubes with EDTA (BD Vacutainer, NJ, USA). Brains were rapidly removed and kept on ice for rapid dissection of several brain regions (Glowinski & Iversen 1966) for Pb analysis.

Blood samples of 200 μl were added to 800 μl of 30% suprapur $HNO_3$ (Merck, Edo. de Mex., Mexico) and centrifuged at 18,500 ***g*** (15 min). From the clear solution, 100-μl aliquot was taken and diluted (1:5 v/v) with deionized water.

Tissue samples of brain regions were weighed, placed in polypropylene tubes and digested in 1 ml of concentrated $HNO_3$ suprapur (Merck) in a shaking water bath at 60 °C for 30 min. Thereafter, a 100-μl aliquot was taken from the clear solution and diluted (1/5 v/v) with deionized water. Diluted samples of blood and brain regions were injected into an atomic absorption spectrophotometer (Model 3110; Perkin-Elmer, Norwalk, CT, USA) with graphite furnace (HGA-600) and auto-sampler (AJS60) adjusted to a wavelength of 283.3 nm. For each analysis, quality control standards (Wisconsin State Laboratory of Hygiene, Madison, WI, USA) and calibration curves (constructed by adding known amounts of Pb standard; Merck, Darmstadt, Germany) were determined at the beginning and end of the sample run to optimize conditions and validate the results. Blood Pb results were expressed as μg of Pb/dl blood, and the content of Pb in brain regions was expressed as μg of Pb/g tissue wet weight.

### *Animal perfusion, tissue processing and immunohistochemistry*

At 90 days of age, male rats (five animals per treatment) were randomly selected and anaesthetized with sodium pentobarbital (40 mg/kg, ip; Pfizer) between 12:00–13:00 h to prevent circadian fluctuations. Animals were perfused intracardially with physiological saline for vascular rinse, followed by 4% cold paraformaldehyde in 0.1 M phosphate-buffered saline (PBS) at pH 7.4, with a continuous infusion pump (Masterflex, Vernon Hills, IL, USA). After perfusion, each brain was dissected carefully from the cranial cavity and postfixed for 3 h in fresh fixative at 4 °C and rinsed in PBS. Small blocks of tissue containing the anterior hypothalamus were cryoprotected in solutions of 15% and 30% sucrose in 0.1 M PBS until they sank. These tissue samples were subsequently sectioned in coronal plane at 40 μm thickness with a cryostat (CM1850, Leica Microsystems, Nussloch GmbH, Germany). Alternate sections were separately collected in PBS, to obtain four independent sets of sections from each brain. Each set was then processed for VIP, VP or GFAP immunostaining. To show cellular bodies, another set was stained with Cresyl Violet acetate (Sigma, St. Louis, MO, USA).

Free-floating sections from each animal were treated with 0.3% hydrogen peroxide (Merck, Germany) solution for 10 min to inhibit endogenous peroxidase activity and later with 1% Triton x-100 (Sigma) in PBS for 10 min. Non-specific binding sites were blocked by incubation in 5% bovine serum albumin (BSA; Amersham Biosciences, Buckinghamshire, UK) and 1% Triton X-100 in PBS (BSA-TX-PBS) for 2 h at room temperature. The floating sections were incubated with rabbit-polyclonal antibodies against VIP, VP or GFAP (Biomeda, Foster City, CA, USA), at a dilution of 1:500 in BSA-TX-PBS, for 48 h at 4 °C. Then, the sections were incubated for 1 h at room temperature with biotinylated anti-rabbit IgG (DAKO, Carpinteria, CA, USA). The sections were subsequently incubated with streptavidin–horseradish peroxidase (DAKO) for 1 h at room temperature. Immunoreactivity was visualized with the diaminobenzidine reaction (DAKO). Three 10-min washes in 0.1 M PBS were performed between steps. The sections were mounted on poly-L-lysine (Sigma)-coated slides, air-dried, cleared with xylene and coverslipes were applied with entellan (Merck). All tissue sections from control and experimental animals were processed at the same time and in parallel to minimize any potential variance in staining procedure.

### *Morphometric analysis*

Morphometric analysis was manually performed using a computerized image analysis system (Metamorph, version 4.5; Molecular Devices, Downington, PA, USA) attached to a light microscope (DMLS, Leica Microsystems, GmbH Wetzlar, Germany). Two representative sections from the middle level of the SCN were selected of each animal, corresponding approximately to anterioposterior −1.3 mm from bregma (Paxinos & Watson 1998). Slides from two groups were randomized and coded such that all subsequent analyses were blindly conducted. The anatomical borders of the SCN were delimited with phase-contrast microscopy. The area of the SCN was measured at ×20, and the number of cells in the SCN area was counted at ×60. The criterion to manually select the targets to be counted was a minimum ratio of background to immunoreactivity of 1:3 in OD. Cellular density was expressed in 1000 $\mu m^2$ (estimated from the number of targets counted and the area of the region from which they were collected).

Twenty well-delimited neuronal bodies, in which the cell nucleus could be clearly identified, were randomly chosen and outlined manually in each animal for the measurement of VP- or VIP-immunoreactive neurons. On each cell chosen for study, the major and minor axes and somatic area were determined. Previous studies have shown that OD measurements reflect changes in protein expression parallel to those obtained using a biochemical protein assay such as Western blot (Mufson *et al.* 1997). Therefore, in these same cells, the OD, expressed as arbitrary OD units, was determined (Rojas *et al.* 2005) at ×100. Cellular OD was expressed in 100 $\mu m^2$. Furthermore, OD in the SCN of

VIP- and VP-immunoreactive sections was determined at ×20 and expressed in 10 000 $\mu m^2$. Owing to the fact that glial cells increase the expression of GFAP in the case of toxicity by Pb (Selvín-Testa *et al.* 1991), the OD of the astrocytes was determined in tissue sections that were processed for GFAP immunostaining. However, because of the difficulty in delimiting the outline of glial cytoskeleton with image analysis system, we decided to determine the OD in the area occupied by SCN (at ×20 and expressed in 10 000 $\mu m^2$).

### *Statistical analysis*

Data are expressed as mean ± SEM and were analysed by using one-way analysis of variance (ANOVA). Values of $P < 0.001$, $P < 0.01$ or $P < 0.05$ were considered significant. The brain regions were analysed with Tukey's test. Values of $P < 0.05$ were considered significant.

## Results

### *Body and brain weights*

At 90 days of age, no significant difference was found between control and experimental groups in the body weight (one-way ANOVA: $F = 0.2_{[df = 1,8]}$, $P > 0.05$; 544.8 ± 19.8, 533.6 ± 13.5, respectively) and brain weight (one-way ANOVA: $F = 1.8_{[df = 1,8]}$, $P > 0.05$; 2.1 ± 0.1, 2.1 ± 0.3, respectively).

### *Pb levels in blood and brain regions*

The developmental Pb dosing regimen used in the present experiments caused significant increases in metal in blood and brain regions. Blood Pb level was significantly increased by 14-fold when compared with the control group (one-way ANOVA: $F = 204.4_{[df = 1,8]}$, $P < 0.001$). The content of Pb in hypothalamus, hippocampus and prefrontal cortex was significantly increased by 8.4-fold (one-way ANOVA: $F = 229.9_{[df = 1,8]}$, $P < 0.001$), 11.7-fold (one-way ANOVA: $F = 661.6_{[df = 1,8]}$, $P < 0.001$) and 10.5-fold (one-way ANOVA: $F = 418.9_{[df = 1,8]}$, $P < 0.001$), respectively, in the Pb-treated animals compared with the control group (Table 1). In the Pb-exposed group, the content of this metal in prefrontal cortex and hypothalamus was significantly increased, compared with hippocampus ($P < 0.05$).

### *SCN cytoarchitecture*

Anatomical distribution of VP-, VIP- and GFAP-immunoreactive cells in the SCN was similar in control and experimental animals. Vasopressin immunoreactive neurons were observed in the shell (dorsomedial) subdivision. A few immunoreactive neurons were scattered in the core (ventrolateral) region of the SCN. VIP-immunoreactive neurons were located in the area of the SCN immediately adjacent to optic chiasm (core region). The soma of some of the neurons was scattered in the dorsal region of the SCN. Some VP- and VIP-immunoreactive neurons were entirely embedded within the optic chiasm. GFAP-immunoreactive cells were distributed throughout SCN, but especially in the ventrolateral region. The middle level of the SCN stained for VP, VIP, GFAP and Nissl stain in control and experimental animals is shown in Figure 1.

**Table 1** Effects of chronic early lead (Pb) exposure (320 ppm, prenatal and postnatal) on the Pb levels in blood and brain regions of rats of 90 days of age

| | Concentration of Pb | |
|---|---|---|
| Sample | Control group | Pb-exposed group |
| Blood (μg/dl) | 2.1 ± 0.2 | 29.5 ± 1.9* |
| Frontal cortex (μg/g tissue) | 6.6 ± 0.3 | 69.1 ± 3.0* |
| Hypothalamus (μg/g tissue) | 7.8 ± 0.3 | 65.5 ± 3.8* |
| Hippocampus (μg/g tissue) | 4.7 ± 0.3 | 53.8 ± 1.9*† |

Data were obtained from five animals per group and are expressed as means ± SEM. *Statistically significant difference compared with control group, $P < 0.001$, one-way ANOVA. †Statistically significant difference when compared to prefrontal cortex and hypothalamus of the group exposed to Pb.

### *Morphometric analysis*

Table 2 shows the effects of CePbe on the cellular density, morphology and OD of the cells in the SCN. Results from the morphometric analysis of cellular density showed a significant decrease in the animals exposed to Pb compared with the control group [VIP, one-way ANOVA: $F = 12.5_{[df = 1,8]}$, $P < 0.01$, (−22.4%); VP, one-way ANOVA: $F = 18.1_{[df = 1,8]}$, $P < 0.01$, (−16.7%); GFAP, one-way ANOVA: $F = 10.6_{[df = 1,8]}$, $P < 0.05$, (−18.5%); Nissl stain, one-way ANOVA: $F = 8.9_{[df = 1,8]}$, $P < 0.05$, (−19.7%)]. Chronic early Pb exposure induced significant increases in the minor and major axes and somatic area of VIP- [one-way ANOVA: $F = 6.4_{[df = 1,198]}$, $P < 0.05$, (7.5%); one-way ANOVA: $F = 15.7_{[df = 1,198]}$, $P < 0.001$, (10.1%); one-way ANOVA: $F = 16.4_{[df = 1,198]}$, $P < 0.001$, (18.7%), respectively] and VP- [one-way ANOVA: $F = 7.4_{[df = 1,198]}$, $P < 0.01$, (4.9%); one-way ANOVA: $F = 22.0_{[df = 1,198]}$, $P < 0.001$, (11.2%); one-way ANOVA: $F = 21.8_{[df = 1,198]}$, $P < 0.001$, (19.4%), respectively) immunoreactive neurons. The densitometric analysis of VIP-immunoreactive cells in SCN showed a significant increase in the experimental group [one-way ANOVA: $F = 7.0_{[df = 1,198]}$, $P < 0.01$, (17.8%)] compared with the control group. However, no statistical difference was found in the OD of VP-immunoreactive cells between control rats and animals exposed to Pb [one-way ANOVA: $F = 2.9_{(df = 1,198)}$, $P > 0.05$, (10.2%)] The OD in the SCN of tissue sections processed for VIP immunostaining was significantly increased in the experimental group [one-way ANOVA: $F = 5.7_{(df = 1,8)}$, $P < 0.05$, (36.4%)]. No significant difference was found in OD of the SCN in tissue sections immunostained for VP (one-way

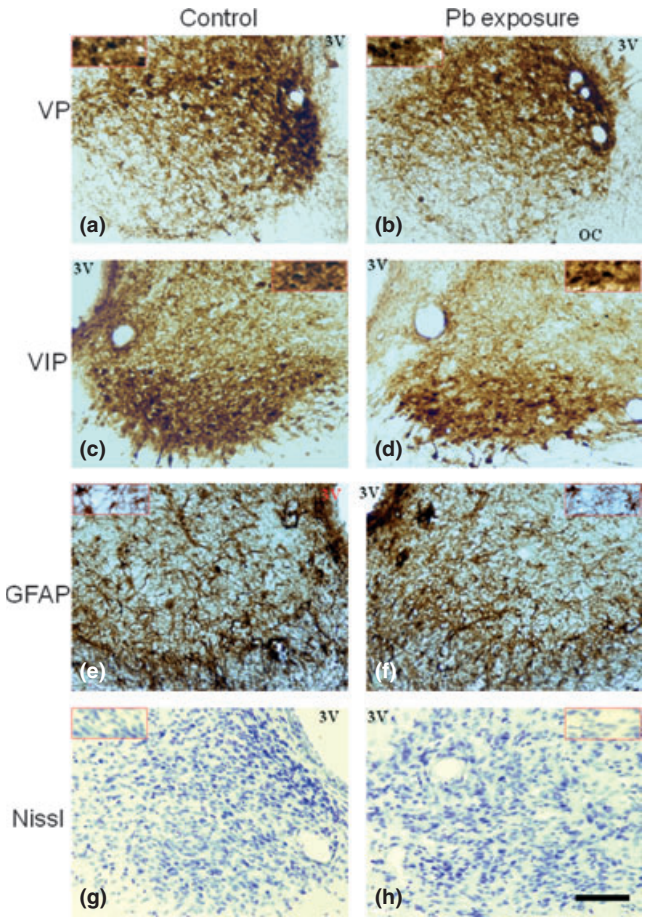


**Figure 1** Histological images of coronal sections of suprachiasmatic nucleus of rat at the middle level at 90 days of age. Immunohistochemistry for vasopressin (VP), vasoactive intestinal polypeptide (VIP) and glial fibrillar acidic protein (GFAP), and sections stained with Cresyl Violet (Nissl) of control animals (a, c, e and g) and animals subjected to chronic early lead (Pb) exposure (320 ppm, prenatal and postnatal) (b, d, f and h). (a–f) There are no visible differences in the anatomical distribution of immunoreactivity pattern between both groups. Sections of 40 μm thickness. Calibration bar 100 μm. The inserts show a magnification view (×60). 3V, third ventricle; OC, optic chiasm. ×20.

ANOVA: $F = 3.1_{(df = 1,8)}$, $P > 0.05$, 14.8%) and GFAP [one-way ANOVA: $F = 1.8_{(df = 1,8)}$, $P > 0.05$, 15.4%].

## Discussion

It has been established that development of the central nervous system is more vulnerable to Pb effects than adult brain because of the not fully developed blood–brain barrier and defence mechanisms. Deane and Bradbury (1990) reported that Pb crosses the blood–brain barrier of adult brain. This suggests that the central nervous system is a target for Pb in children and adults.

In this study, developmental Pb exposure resulted in an increase in Pb levels in the blood and a marked accumulation of Pb in the brain regions analysed. These suggest the free access of the metal from the environment to the blood and brain. In the group exposed to Pb, prefrontal cortex and hypothalamus significantly accumulated more Pb, when compared to hippocampus. This shows that the SCN is a preferential target for Pb. Several studies reported that damage produced by Pb occurs preferentially in the hippocampus, prefrontal cerebral cortex (Finkelstein *et al.* 1998) and hypothalamus (Wang *et al.* 2006) as shown in the current study.

It has been reported that Pb exposure disrupts the temporal organization of behavioural patterns (Shafiq-ur-Rehman 1999), circadian rhythm of locomotor activity (Collins *et al.* 1984; Shafiq-ur-Rehman *et al.* 1986; Rojas-Castañeda *et al.* 2007) and sleep-wake cycle (Kumar & Desiraju 1992). These disruptions ultimately alter the ability of the organism to cope and interact with its environment. To our knowledge, this is the first morphological evidence of Pb-induced abnormalities on the cells of circadian pacemaker. The size of cell bodies and the complexity of the dendritic tree in maturing granule cells have been shown to correlate with changes in their electrophysiological properties (Liu *et al.* 2000). Our data indicate that CePbe induces a significant increase in the minor and major axes and somatic area of VIP- and VP-immunoreactive neurons. These morphometric results show alterations in the morphology of the neurons of the SCN, which could alter its functional properties.

The significant decrease in the density of VIP and VP neurons in animals exposed to Pb during development may be due, at least in partial way, to: (i) decrease in antioxidant enzymes and an increase in oxidative stress, induced by free radicals leading to lipid peroxidation with damage to the cytoplasmic membranes (Villeda-Hernández *et al.* 2001; Prasanthi *et al.* 2010); (ii) apoptosis, in several brain regions of the central nervous system (Han *et al.* 2007; Kumar *et al.* 2009; Sharifi *et al.* 2010); (iii) inflammatory factors released by glia may result in neuronal death (Chao *et al.* 1995; Liu *et al.* 2000) and (iv) reduction in intracellular level of VIP or VP in SCN cells that would preclude detection by immunostaining because of subthreshold amounts of antigen/epitope, as a consequence of changes in the metabolism. The results of the present investigation suggest that CePbe induces a significant decrease in the cellular density in Nissl-stained SCN slices. This mainly suggests a direct loss of cells.

A decrease in the number of cells may affect the innervation of the SCN and/or alter its afferents/efferents pathways. This can contribute to the generation of morphological and functional alterations of the SCN and/or affect the function of peripheral clocks. Chronic Pb exposure has been shown to decrease the number of neurons of the hippocampus (Han *et al.* 2007), to reduce dendritic branching and to decrease synaptic density and development (Verina *et al.* 2007).

Previous report showed that astroglia can accumulate and store Pb (Tiffany-Castiglioni *et al.* 1986). Accumulation of Pb may provide the mechanism that protects neurons that

**Table 2** Effects of chronic early lead (Pb) exposure (320 ppm, prenatal and postnatal) on morphometric parameters of vasoactive intestinal polypeptide (VIP), vasopressin (VP) and glial fibrillar acidic protein (GFAP) immunoreactive cells and stained neurons with Nissl in the suprachiasmatic nucleus (SCN) of rats at 90 days of age

| Group | | Cellular density (1000 μm$^2$) | Minor axis (μm) | Major axis (μm) | Somatic area (μm$^2$) | Cellular optical density (100 μm$^2$) (arbitrary units) | Optical density in the SCN (10 000 μm$^2$) (arbitrary units) |
|---|---|---|---|---|---|---|---|
| VIP | Control | 5.8 ± 0.2 | 6.7 ± 0.1 | 9.9 ± 0.2 | 40.7 ± 1.2 | 0.45 ± 0.02 | 0.030 ± 0.003 |
| | Pb | 4.5 ± 0.3** | 7.2 ± 0.1* | 10.9 ± 0.2*** | 48.3 ± 1.5*** | 0.53 ± 0.03* | 0.040 ± 0.003* |
| VP | Control | 6.0 ± 0.2 | 6.1 ± 0.1 | 8.9 ± 0.1 | 32.4 ± 0.9 | 0.49 ± 0.02 | 0.034 ± 0.002 |
| | Pb | 5.0 ± 0.1** | 6.4 ± 0.1** | 9.9 ± 0.2*** | 38.7 ± 1.0*** | 0.54 ± 0.02 | 0.039 ± 0.001 |
| GFAP | Control | 2.7 ± 0.1 | | | | | 0.13 ± 0.01 |
| | Pb | 2.2 ± 0.1* | | | | | 0.15 ± 0.01 |
| Nissl | Control | 13.2 ± 0.3 | | | | | |
| | Pb | 10.6 ± 0.8* | | | | | |

Results are expressed as mean ± SEM of 5 animals per group. Statistically significant difference compared with control group: *$P < 0.05$; **$P < 0.01$; ***$P < 0.001$, one-way ANOVA.

are more sensitive than astroglia to the toxic effects of Pb (Tiffany-Castiglioni 1993). However, such storage of Pb in astroglia may provide a reservoir for its continuous release and thereby may contribute to the toxicity of adjacent neurons or glia themselves (Struzynska 2009). Under several pathological conditions, including chronic toxicity by Pb, glial cells undergo rapid changes, example of which is the increased expression of GFAP (Selvín-Testa *et al.* 1991), which have been described as reactive gliosis. In activated form, glia may generate and/or maintain the inflammatory reaction in brain by producing interleukin (IL)-1β, IL-6 and tumour necrosis factor-α, (Zhao & Schwartz 1998). It is postulated that these inflammatory factors released by glia contribute to the destructive processes resulting in neuronal cell death (Chao *et al.* 1995; Liu *et al.* 2000). This could be associated, at least in partial form, with the decrease in the cellular density observed in this work.

The circadian pacemaker is regarded as a multioscillatory system, in such a way that neurons are considered independent oscillators, whose coupling may determine the output of the circadian system (Welsh *et al.* 1995; Miller 1998). A coupling mechanism must exist among the individual neurons of the SCN, to generate a robust 24-h collective self-sustained rhythm under constant environmental conditions. Several candidate coupling factors, such as VIP and astrocytes (Prosser *et al.* 1994; Aton & Herzog 2005), have been implicated in this mechanism. Therefore, a decrease in the neuronal density and alterations in the intracellular level of VIP and VP, and/or a decrease in the number of GFAP cells and abnormalities of its function, could involve alterations in the function of circadian pacemaker.

In this study, we observed that CePbe resulted in a significant increase in the OD level of VIP in the SCN. This result could be associated with significant increases in both soma size and cellular optical density in animals exposed to Pb in response to a significant decrease in the cellular density. There was a non-significant enhancement in the OD of VP, per neuron and in the SCN, after Pb administration. However, we found a significant increase in the cellular size in this brain region in the same experimental group. These results may be related to a significant decrease in the cellular density. Therefore, the expression of VIP was significantly increased in the experimental group and the expression of VP was similar in control and experimental groups. This might be related to the alterations in the synthesis and release of proteins. Our results suggest neuronal plasticity mechanisms as well as a specific response in different regions of the SCN. In particular, the most vulnerable is the core region. Therefore, this suggests a higher vulnerability for VIP neurons in relation to the VP cells, after Pb exposure, as reported for other environmental factors that affect the developing VP and VIP cells in the SCN (Rojas-Castañeda *et al.* 2008). Each brain region or subregion has different metabolic activity, and the morphometric alterations observed in this study may be secondary to metabolic changes initiated by exposure to Pb.

VIP cells receive photic information directly through the retino-hypothalamic tract, and this information is relayed to the VP cells. Interplay between these two cellular types is responsible for the output of circadian information from the SCN (Antle & Silver 2005). Therefore, alterations in VIP cells can induce disorders in the transmission of photic information in SCN. These alterations could be related to disorders in the onset of locomotor activity (in the phase transition of light/dark cycle) in rats chronically exposed to lead (Rojas-Castañeda *et al.* 2007). The levels of VIP and VP in the SCN are crucial for the maintenance of rhythmic functions, and these levels have a circadian rhythm. VP level shows a peak (acrophase) during the light phase, while the level of VIP shows an acrophase during dark phase (Van Esseveldt *et al.* 2000). In addition, changes observed in circadian rhythms associated with Pb exposure might be related to possible changes in the acrophase and/or phase of expression of VIP and/or VP in the SCN. Further studies are needed to investigate whether the circadian rhythms in the levels of VIP and VP in the SCN are altered by exposure to Pb.

In our study, cellular GFAP immunoreactivity displayed a normal pattern of anatomical distribution in the SCN of animals exposed to Pb. A significant decrease in cellular density of astrocytes in the SCN was observed, and this deficiency may contribute to alterations in function of the circadian pacemaker. We determined a non-significant increase in OD (calculated on the area occupied by the SCN, not by each cell) that may be related to the significant decrease in the number of astrocytes in the SCN induced by the CePbe.

On the other hand, a developmental delay of astrocytes has been postulated to occur after CePbe (Buchheim *et al.* 1994), which can explain the decreased number of astrocytes without discarding the effects of apoptosis on the astrocytes.

Our findings suggest that CePbe induces abnormalities in the density and morphology of the cells of circadian pacemaker, as well as possible disorder in the levels of VIP and VP. These alterations provide a morphological and cellular substrate underlying circadian alterations previously reported in animals with exposure to chronic Pb.

## Acknowledgements

The authors thank Pedro Medina for his assistance in the vivarium. This work was supported by a CONACYT (164490) fellowship to Julio César Rojas-Castañeda.

## References

Antle M.C. & Silver R. (2005) Orchestrating time: arrangements of the brain circadian clock. *Trends Neurosci.* **28**, 145–151.

Aton S.J. & Herzog E.D. (2005) Come together, right… now: synchronization of rhythms in a mammalian circadian clock. *Neuron* **48**, 531–534.

Buchheim K., Noack S., Stoltenburg G., Lilienthal H., Winneke G. (1994) Developmental delay of astrocytes in hippocampus rhesus monkeys reflects the effect of pre- and postnatal chronic low level lead exposure. *Neurotoxicology* **15**, 665–669.

Chao C.C., Hu S., Peterson P.K. (1995) Glia, citokines, and neurotoxicity. *Crit. Rev. Neurobiol.* **9**, 189–205.

Collins M.F., Hrdina P.D., Whittle E., Singhal R.L. (1984) The effects of low-level lead exposure in developing rats: changes in circadian locomotor activity and hippocampal noradrenaline turnover. *Can. J. Physiol. Pharmacol.* **62**, 430–435.

Deane R. & Bradbury M.W.B. (1990) Transport of lead-203 at the blood-brain barrier during short cerebrovascular perfusion with saline in the rat. *J. Neurochem.* **54**, 905–914.

Finkelstein Y., Markowitz M.E., Rosen J.F. (1998) Low-level lead-induced neurotoxicity in children: an update on central nervous system effects. *Brain Res. Brain Res. Rev.* **27**, 168–176.

Glowinski J. & Iversen L.L. (1966) Regional studies of catecholamine in the brain. I. The disposition of 3H-norepinefrine, 3H-dopamine, and 3H-Dopa in various regions of the brain. *J. Neurochem.* **13**, 655–659.

Han J.M., Chang B.J., Li T.Z. *et al.* (2007) Protective effects of ascorbic acid against lead- induced apoptotic neurodegeneration in the developing rat hippocampus *in vivo*. *Brain Res.* **1185**, 68–74.

Hastings M.H. & Herzog E.D. (2004) Clock genes, oscillators, and cellular networks in the suprachiasmatic nuclei. *J. Biol. Rhythms* **19**, 400–413.

Hastings M., O'Neil J.S., Maywood E.S. (2007) Circadian clocks: regulators of endocrine and metabolic rhythms. *J. Endocrinol.* **195**, 187–198.

Karatsoreos I.N. & Silver R. (2007) Minireview: the neuroendocrinology of the suprachiasmatic nucleus as a conductor of body time in mammals. *Endocrinology* **148**, 5640–5647.

Kumar M.V. & Desiraju T. (1992) EEG spectral power reduction and learning disability in rats exposed to lead through postnatal developing age. *Indian J. Physiol. Pharmacol.* **36**, 15–20.

Kumar B.K., Rao Y.P., Noble T.O. *et al.* (2009) Lead-induced alteration of apoptotic proteins in different regions of adult rat brain. *Toxicol. Lett.* **184**, 56–60.

Lasley S.M. & Gilbert M.E. (2002) Rat hippocampal glutamate and GABA release exhibit biphasic effects as a function of chronic lead exposure level. *Toxicol. Sci.* **66**, 139–147.

Liu X., Tilwalli S., Ye G., Lio P., Pasternak J.F., Trommer B.L. (2000) Morphologic and electrophysiologic maturation in developing dentate gyrus granule cells. *Brain Res.* **856**, 202–212.

Miller J.D. (1998) The SCN is comprised of a population of coupled oscillators. *Chronobiol. Int.* **15**, 489–512.

Mufson E.J., Lavine N., Jaffar S., Kordower J.H., Quirino R., Saragovi H.U. (1997) Reduction in p140-TrkA receptor protein within the nucleus basalis and cortex in Alzheimer's disease. *Exp. Neurol.* **146**, 91–103.

Paxinos G. & Watson C. (1998) *The Rat Brain in Stereotaxic Coordinates*, 4th edn. San Diego, California: Academic Press.

Prasanthi R.P., Devi C.B., Basha D.C., Reddy N.S., Reddy G.R. (2010) Calcium and zinc supplementation protects lead (Pb)-induced perturbations in antioxidant enzymes and lipid peroxidation in developing mouse brain. *Int. J. Devl. Neurosci.* **28**, 161–167.

Prosser R.I., Edgar D.M., Heller H.C., Miller J.D. (1994) A possible glial role in the mammalian circadian clock. *Brain Res.* **643**, 296–301.

Reppert S.M. & Weaver D.R. (2002) Coordination of circadian timing in mammals. *Nature* **418**, 935–941.

Rojas P., Franco-Perez J.E., Rojas C. *et al.* (2005) Reduction of zinc-positive terminal fields in striatum of mouse after 1-methyl-4-phenylpyridinium neurotoxicity. *Neurotoxicology* **26**, 959–968.

Rojas-Castañeda J.C., Vigueras-Villaseñor R.M., Escobar C., Rios C. (2007) Alteraciones inducidas por la exposición crónica a plomo sobre la morfología y función del núcleo supraquiasmático de la rata. 1ª. Reunión bienal de investigación pediátrica, 37.

Rojas-Castañeda J., Vigueras-Villaseñor R.M., Rojas P., Rojas C., Cintra L. (2008) Immunoreactive vasoactive intestinal polypeptide and vasopressin cells after a protein malnutrition diet in the suprachiasmatic nucleus of the rat. *Lab. Anim.* **42**, 360–368.

Selvín-Testa A., Lopez-Costa J.J., Nessi de Aviñon A.C., Pecci Saavedra J. (1991) Astroglial alterations in rat hippocampus during chronic lead exposure. *Glia* **4**, 384–392.

Shafiq-ur-Rehman (1999) Circadian rhythm of stereotyped complex behaviours in rats in environmental lead exposure. *Prog. Neuropsychopharmacol. Biol. Psychiatry* **23**, 149–159.

Shafiq-ur-Rehman, Khushnood-ur-Rehman, Kabir-ud-Din, Chandra O. (1986) Differential effects of chronic lead intoxication on circadian rhythm of ambulatory activity and on regional brain norepinephrine levels in rats. *Bull. Environ. Contam. Toxicol.* **36**, 81–91.

Sharifi A.M., Mousavi S.H., Jorjani M. (2010) Effect of chronic lead exposure on pro-apoptotic Bax and anti-apoptotic Bcl2 protein

expression in rat hippocampus *in vivo*. *Cell. Mol. Neurobiol.* **30**, 769–774.

Struzynska L. (2009) A glutamatergic component of lead toxicity in adult brain: The role of astrocytic glutamate transporters. *Neurochem. Int.* **55**, 151–156.

Tho K.L. (2008) Basic Science Review on circadian rhythm biology and circadian sleep disorders. *Ann. Acad. Med. Singapore* **37**, 662–668.

Tiffany-Castiglioni E. (1993) Cell culture models for lead toxicity in neuronal and glial cells. *Neurotoxicology* **14**, 513–536.

Tiffany-Castiglioni E., Zmudzki J., Bratton G.R. (1986) Cellular targets of lead neurotoxicity: *in vitro* models. *Toxicology* **42**, 305–315.

Toscano C.D., Hashemzadeh-Gargari H., McGlothan J.L., Guilarte T.R. (2002) Developmental $Pb^{2+}$ exposure alters NMDAR subtypes and reduces CREB phosphorylation in the rat brain. *Dev. Brain Res.* **139**, 217–226.

Van Esseveldt K.E., Lehman M.N., Boer G.J. (2000) The suprachiasmatic nucleus and the circadian time-keeping nucleus and the circadian time-keeping system revisited. *Brain Res. Brain Res. Rev.* **33**, 34–77.

Verina T., Rhode C.A., Guilarte T.R. (2007) Environmental $Pb^{2+}$ exposure during early life alters granule cell neurogenesis and morphology in the hippocampus of young adult rats. *Neuroscince* **145**, 1037–1047.

Verstraeten S.V., Aimo L., Oteiza P.I. (2008) Aluminium and lead: molecular mechanisms of brain toxicity. *Arch. Toxicol.* **82**, 789–802.

Villeda-Hernández J., Barroso-Moguel R., Mendez-Armenta M., Nava-Ruiz C., Huerta-Romero R., Rios C. (2001) Enhanced brain regional lipid peroxidation in developing rats exposed to low level lead acetate. *Brain Res. Bull.* **55**, 247–251.

Wang J., Wu J., Zhang Z. (2006) Oxidative stress in mouse brain exposed to lead. *Ann. Occup. Hyg.* **50**, 405–409.

Welsh D.K., Logothetis D.E., Meister M., Reppert S.M. (1995) Individual neurons dissociated from rat suprachiasmatic nucleus express independently phased circadian firing rhythms. *Neuron* **14**, 697–706.

Winneke G. (1996) Inorganic lead as a developmental neurotoxicant: some basic issues and the Düsseldorf experience. *Neurotoxicology* **17**, 565–580.

Yan L. & Okamura H. (2002) Gradients in the circadian expression of Per 1 and Per 2 genes in the rat suprachiasmatic nucleus. *Eur. J. Neurosci.* **15**, 1153–1162.

Yan L. & Silver R. (2002) Differential induction and localization of mPer1 and mPer2 during advancing and delaying phase shifts. *Eur. J. Neurosci.* **16**, 1531–1540.

Zhao B. & Schwartz J.P. (1998) Involvement of cytokines in normal CNS development and neurological diseases: recent progress and perspectives. *J. Neurosci. Res.* **52**, 7–16.